Formation of interfaces between In and Au and GaAs(100) studied with soft-x-ray photoemission spectroscopy

D. Mao, M. Santos, M. Shayegan, and A. Kahn
Department of Electrical Engineering, Princeton University, Princeton, New Jersey 08544

G. Le Lay
Campus de Luminy and Université de Provence, Marseille, France

Y. Hwu
Department of Physics and Synchrotron Radiation Center, University of Wisconsin, Madison, Wisconsin 53706

G. Margaritondo
Institut de Physique Appliquée, Ecole Polytechnique Fédérale, CH-1015 Lausanne, Switzerland

L. T. Florez and J. P. Harbison
Bellcore, Red Bank, New Jersey 07701-7040
(Received 2 August 1991)

A study of the formation of In- and Au-GaAs(100) interfaces is reported. The metal overlayers are deposited in ultrahigh vacuum on room-temperature (RT) and low-temperature (LT) (100)GaAs grown by molecular-beam epitaxy, following the evaporation of a protective As capping layer from the semiconductor surface. High-resolution photoemission spectroscopy and low-energy electron diffraction are used to characterize these interfaces. In forms a two-dimensional interface layer plus clusters at RT and LT, with reduced clustering at LT. The top substrate layers are only slightly altered by In. The Au-induced perturbation is more significant, as reflected by Ga outdiffusion even at LT. Different Ga core-level components are found at RT and LT, attesting to different levels of segregation as a function of temperature. The GaAs(100) band bending is studied as a function of metal coverage and deposition temperature. Kelvin-probe measurements, coupled with synchrotron-radiation photoemission, are performed to evaluate the synchrotron-light-induced surface photovoltage. The Fermi level is found to be pinned at 0.4 and 0.6 eV above the valence-band maximum for Au and In, respectively, in good agreement with the positions obtained on the cleaved (110) GaAs surface. Evidence of correlation between pinning and overlayer metallization is found for both interfaces.

I. INTRODUCTION

As most III-V-based devices are fabricated on (100) surfaces, photoemission measurements of the initial stages of the formation of Schottky barriers have been extended to metal-GaAs(100) interfaces during the past few years.[1–7] This provides valuable points of comparison with results obtained from (110) interfaces.[8–10] One can argue, for example, that Fermi level (E_F) pinning mechanisms based on surface defects[10] and interface chemistry,[11] which are specific of the starting surface, should depend much more on surface orientation than mechanisms based on gap states induced[12–14] or modified[15] by the metal, which derive from more general properties of metal-semiconductor contacts. Furthermore, thin overlayers are known to exhibit smoother morphologies on the (100) surface than on the cleaved and inert (110) surface where submonolayer clustering is often seen. The local conformation of the adatom in the early stages of overlayer formation should bear directly on the type of gap state it induces on the surface. Thus, a comparison of the evolution of the band bending as a function of metal coverage on these two types of surfaces should help identify dominant E_F pinning mechanisms.

The work of Viturro *et al.*[1,2] on Schottky barriers formed on (100) *n*-type GaAs surfaces grown by molecular-beam epitaxy (MBE) has produced controversial results which so far have not been independently reproduced.[3,5,7] Various metals with low (Al,In) and high (Au) work functions evaporated on low-temperature surfaces originally capped with As and decapped at high temperature were found to give a 0.75 eV distribution of the barrier height, suggesting that the Schottky-Mott limit could be approached in these cases. This very large barrier spread is contrary to the results obtained on (110) surfaces, where barrier heights are almost independent of the metal work function (typical barrier height distribution ~ 0.25 eV). These puzzling discrepancies could conceivably originate from subtle differences in the substrate preparation. First, the difference between the densities of bulk defect in MBE and liquid-encapsulated Czochralski materials and their role in the E_F pinning process are still controversial. Second, the quality and stoichiometry of interfaces obtained by decapping MBE-grown surfaces

 ©1992 The American Physical Society

could vary from one laboratory to another, and need to be studied and understood. Finally, the electronic properties of the reconstructed GaAs surface and near-surface atomic layers, which could act as a dielectric separating the metal from the semiconductor,[16] are still unknown and must be investigated. It is also important to note that these results[1,2] were obtained with very low doped *n*-type GaAs MBE layers on which the photoemission process is likely to have induced considerable surface photovoltage (SPV).[17-20] detailed investigations of these types of interfaces, using different substrates and doping conditions, must therefore be performed.

We have used high-resolution soft-x-ray photoemission spectroscopy (SXPS) combined with low-energy electron diffraction (LEED) to study the deposition of Au and In on room temperature (RT) and low temperature (LT) GaAs(100). Care was taken to perform these measurements with sample doping, temperature, and photon flux resulting in negligible SPV. Au and In were chosen because they are typical high and low work function metals, respectively, and have been reported to produce high (~ 1.0 eV) and low (0.25 eV) Schottky barrier heights on decapped LT (100) GaAs.[1] Curve fitting of the high-resolution photoemission spectra provided a detailed picture of the chemical reaction, overlayer growth morphology and band bending at these interfaces. Our main result is that the mechanisms which control the band bending appear to be compatible with those inferred from the work on (110) interfaces, namely, adatom-induced gap states at low coverage and metal-induced gap states at high coverage. The pinning positions of the Fermi level obtained with Au and In also appear to be incompatible with the reported Schottky-Mott limit.

II. EXPERIMENTS

The SXPS measurements were done on the Grasshopper Mark II and Mark V beam lines at the Synchrotron Radiation Center of the University of Wisconsin. The ultrahigh vacuum chamber (base pressure $=8\times 10^{-11}$ Torr) was equipped with a double-pass cylindrical mirror analyzer, an evaporation station and a vibrating Kelvin probe. The Kelvin probe, described in detail elsewhere,[19,20] was used to define experimental conditions under which the SXPS measurements would not be affected by SPV.

All measurements were done with 65-eV synchrotron light and with an estimated light intensity of 10^{10} photons/sec cm^2, corresponding to a maximum photocurrent density of 10^{-7} A/cm^2. Valence-band and high-resolution core-level spectra were recorded to study interface chemistry, overlayer growth mode and band bending. The combined energy resolution of the monochromator and electron analyzer was 0.25 eV in the energy range considered here.

n-type doped (Si, $\geq 10^{18}$ cm^{-3}) and *p*-type doped (Be, $\geq 10^{18}$ cm^{-3}) GaAs layers grown by MBE were capped in the growth chamber with a thick As layer for protection during transfer to the Synchrotron Radiation Center. To prevent degradation of the As cap, the samples were kept in a low vacuum vessel (pressure $\sim 10^{-3}$ Torr) at all times between extraction from the MBE chamber and insertion in the SXPS chamber. The As capping layer was thermally removed in the photoemission chamber by passing current through the thin Mo foil in which the sample was cradled. The annealing temperature was measured with an infrared pyrometer precalibrated with a thermocouple. Decapping was performed in several steps: following the initial annealing at 350° C to remove the bulk of the As cap, the samples were annealed in rapid cycles up to 570 °C to eliminate excess As and bring the surface to a reproducible composition, as measured from the ratio of the height of the As 3*d* and Ga 3*d* core levels taken with 100-eV photons. On all surfaces used in this experiment, this ratio was 1.0 ± 0.05, identical to that obtained on the cleaved (110) surface. The atomic order and geometry on decapped surfaces were studied with LEED. The samples could be cooled to 120 K with a closed cycle He refrigerator. In and Au were evaporated from tungsten baskets. One monolayer (ML) is defined in this work as one adatom per atom of the ideally terminated substrate. For In and Au on (100) GaAs, 1 ML has nominal thicknesses of 1.63 and 1.06 Å, respectively.

III. METHODOLOGY FOR CORE LEVEL ANALYSIS

The Ga 3*d*, As 3*d*, and In 4*d* core-level spectra were analyzed using least-square curve fitting.[21] The parameters are summarized in Table I. The fixed parameters were the spin-orbit splitting and the Lorentzian width (life time) of each core level. The energy separation between the $3d_{5/2}$ Ga and As bulk components ($\Delta E=21.85$ eV) was also fixed in the fitting procedure. The branching ratios for Ga and As were allowed to vary by a maximum of 7% around the statistical value of 1.5. The Gaussian widths of the bulk and surface Ga 3*d* and As 3*d* spectra were kept identical for different metal coverages in all the experiments. Their values were 0.35 and 0.42 eV for Ga 3*d* and As 3*d*, respectively, significantly higher than the instrumental resolution (0.25 eV) because of phonon broadening and possibly other unresolved components due to crystal-field splitting. Additional broadening was allowed for all reacted components. At coverages corresponding to metallic overlayers, Doniach-Šunjić asymmetric line shapes were introduced to account for screening and creation of electron-hole pairs at the Fermi level of the metal.[22]

IV. RESULTS AND DISCUSSION

A. Clean GaAs(100)

Figure 1 shows the (4×2)-$c(8\times 2)$ LEED pattern obtained by decapping the As-covered surface between 500 °C and 570 °C, and corresponding to a nominally Ga-rich composition.[23] A schematic of a missing Ga-dimer row model of the (4×2) unit cell is presented. Some evidence of $\frac{1}{6}$ order spots was also obtained on some of these surfaces. Note that the same reconstruction is obtained for a fairly wide range of decapping temperatures and that the $\frac{1}{6}$ spots appeared only in the high limit of annealing temperatures (generally above 570 °C).

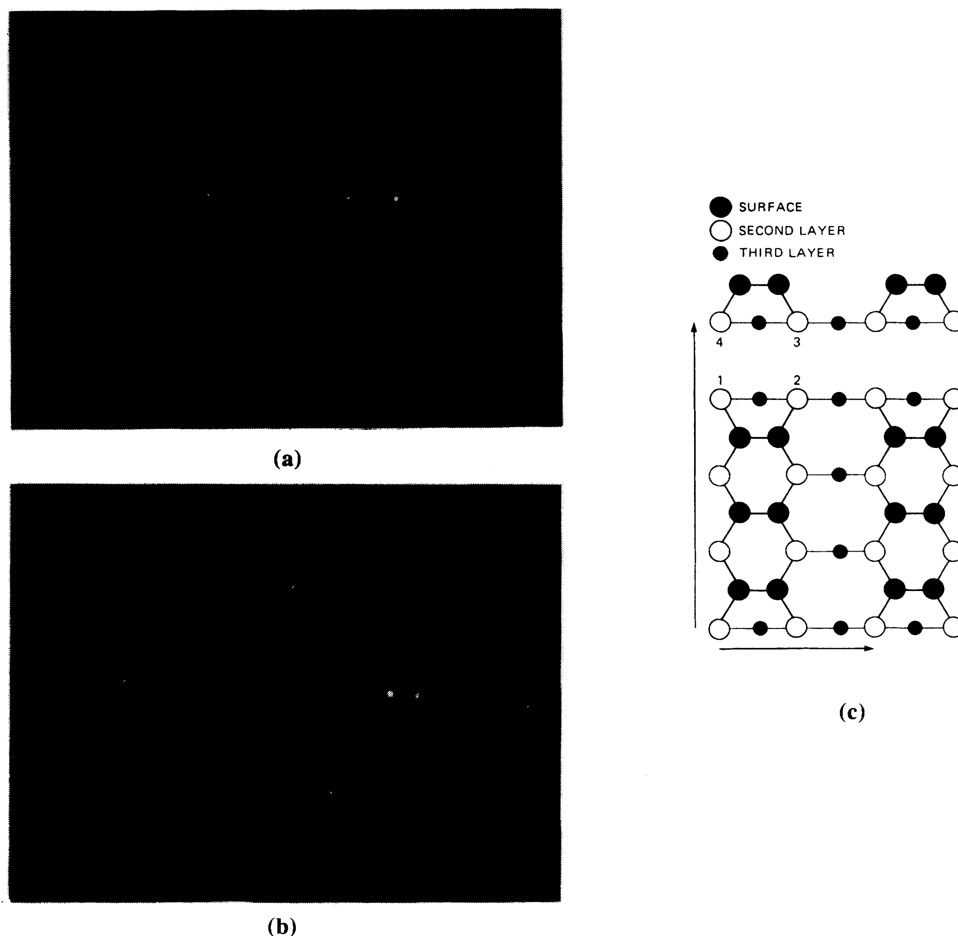

FIG. 1. LEED patterns from the decapped (100) GaAs surface: (a) 500 °C anneal, 70 eV, (b) 555 °C anneal, 60 eV, (c) a schematic of a missing Ga-dimer row model of the (4×2) reconstruction; open and solid circles represent As and Ga atoms, respectively.

The Ga and As core-level spectra of the clean (4×2)-$c(8\times2)$ surface are represented in the top panels of Fig. 2. The details of the curve fitting have been presented elsewhere[24] and are briefly recalled here. All the deconvolution parameters are given in Table I. Three components are necessary to provide an acceptable fit to the Ga core level. The central component B represents photoemission from Ga in a bulklike environment. The high and low binding energy (BE) S_1 and S_2 components have been tentatively attributed to the two inequivalent surface Ga dimers in the (4×2) unit cell.[24] The As core level, on the other hand, can be fitted with just two components, a dominant bulk component B at high BE and a surface component shifted to lower BE. The As surface component has been attributed to the uncovered As atoms of the second layer next to the missing Ga-dimer row (see schematic in Fig. 1). Note that ΔBE between bulk and surface components is almost identical to that found on the (110) surface. Although we can offer only conjectures at this point, it suggests that the conformations of the surface As are similar on both surfaces. In other words, the As is threefold coordinated and sits with a filled dangling bond in a p-like configuration at the top of a three-Ga-based pyramid.

B. In/GaAs(100)

Upon deposition of up to 16 Å In at RT, the substrate reconstruction does not show significant alteration. The overlayer is disordered and does not induce new superstructure. The persistence of the substrate LEED pattern to high coverages results from a growth mode where only the first one-half to one monolayer is two dimensional and clusters form at higher coverage (see below). Since the first 0.5–1 ML In is uniformly distributed over the surface, the persistence of the reconstruction also indicates that the (4×2)-$c(8\times2)$ structure is quite stable and may survive when the surface is entirely covered with In. This should be contrasted with the case of the (110) GaAs surface which is found to be entirely unrelaxed by a uniformly distributed 0.5 ML In deposited at LT.[25]

Figure 2 shows the evolution of the various components of the Ga 3d, In 4d, and As 3d spectra as a function of RT deposition. The fitting parameters for In 4d

TABLE I. Fitting parameters for the Ga 3d and As 3d core-level spectra of a clean GaAs(100) surface taken with 65-eV photons. All energies are in eV.

	Ga 3d	As 3d	In 4d
Spin-orbit splitting	0.45	0.69	0.89
Branching ratio	1.59	1.45	1.50
Gaussian width	0.35	0.42	0.55 (reacted) 0.25 (bulk)
Lorentzian width	0.155	0.17	0.25
BE shift of S_1	0.37	−0.46	
BE shift of S_2	−0.31		

are given in Table I. At low coverage, only one In component is observed at higher BE than metallic In. This component, which has been seen in a previous study by Spindt *et al.*,[4] dominates the In core level up to about 0.5 Å (0.3 ML) where it saturates. Beyond that coverage, a lower BE component emerges. It is substantially narrower than the first one and has an asymmetric line shape beyond 2 Å indicative of emission from a metallic phase (asymmetric parameter equal to 0.10). This is in good agreement with the appearance of a measurable density of states at the Fermi level, as described in Sec. III D.

The high-BE In component is due to isolated In atoms chemisorbed on the surface, i.e., bound to As, or to In in $In_xGa_{1-x}As$ resulting from an In-Ga exchange reaction. Its width reflects the distribution of inequivalent adsorption or reaction sites. This assignment is supported by several facts. First, the energy separation between the high BE component and the metallic component is 0.8 eV, equal to the energy difference between covalently bonded In and metallic In.[26] Second, its intensity increases significantly upon accelerating the In-substrate reaction by annealing the interface at 400 °C (bottom panel of Fig. 2). Finally, a metallic Ga component is resolved at intermediate coverage (Fig. 3), indicating the formation of free Ga upon In-substrate reaction. This metallic Ga component is relatively weak and may appear unnecessary at first glance. However, any attempt to fit the spectrum without this component increases the χ^2 by a factor of 3 and renders the fit visually unacceptable. At higher coverages, the metallic Ga component is buried under the high-intensity In 4d peak.

Similar-core-level spectra, not displayed here, were obtained from the In/GaAs(100) interface formed at LT. The energy position and width of the In peaks are identical to those obtained at RT. Only the relative intensities

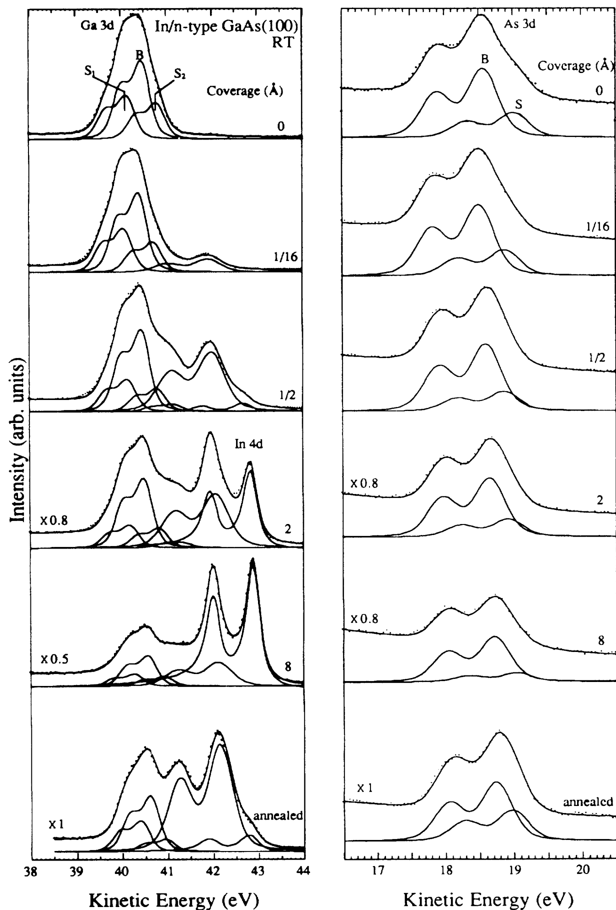

FIG. 2. Ga 3d, In 4d, and As 3d core levels as a function of increasing In coverage on RT n-type GaAs(100). The various components are described in the text. The fitting parameters are given in Table I. The bottom panels correspond to the 8-Å interface annealed at 400 °C. The photon energy is 65 eV.

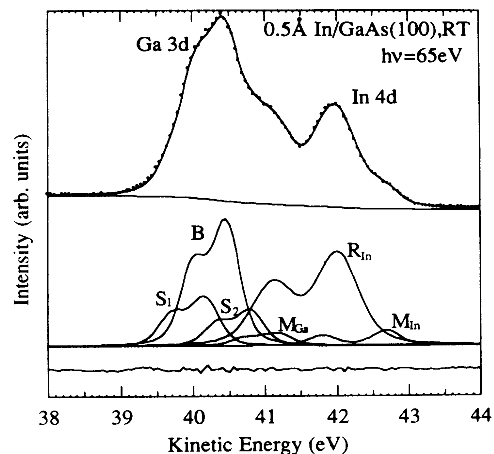

FIG. 3. Decomposition of the Ga 3d and In 4d core levels in bulk Ga (B), two-surface Ga (S_1 and S_2), one metallic Ga (M_{Ga}), one reacted In (R_{In}), and one metallic In (M_{In}) component for 0.5-Å In on RT GaAs(100).

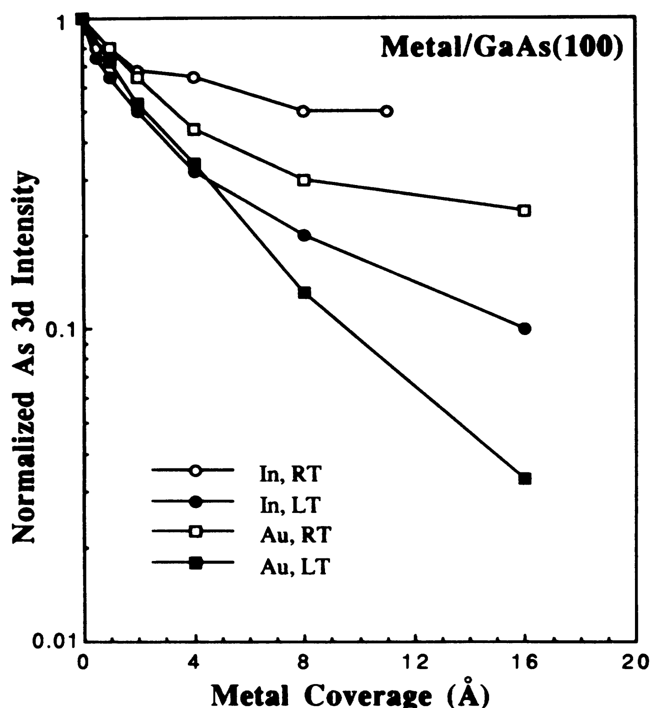

FIG. 4. Integrated As 3d intensity as a function of metal coverage for interfaces between In or Au and GaAs(100) formed at RT and LT.

of the reacted and metallic In peaks are different, as will be discussed below.

The morphology of the In overlayer is deduced from the attenuation of the As 3d intensity plotted against metal coverage (Fig. 4). At RT, deviation from the exponential $e^{-x/\lambda}$ form ($\lambda \sim 4$ Å) occurs only beyond the first monolayer, consistent with a two-dimensional plus cluster growth mode. The first 0.5 Å In is for the most part tightly bound to the substrate. The intensity of the corresponding high-BE component [("reacted" component in Fig. 5(a)], which represents In covalently bound to the substrate or in the first few GaAs layers, saturates beyond 0.5 Å and eventually decreases at the same rate as the substrate signal due to attenuation through the In overlayer. The Ga and As bulk intensities decrease at the same rate, confirming that the slow decay of the substrate signal beyond the first monolayer (Fig. 4) is due to In clustering and not to preferential out diffusion of substrate species (the very small reacted component can be neglected here). The Ga and As surface components persist to high coverage (> 8 Å at RT).

The LT deposition leads to a more laminar growth. The As attenuation deviates from the exponential form only beyond 4 Å, indicating that the first several monolayers are uniformly distributed across the surface. The Ga and As surface components remain visible to 2 Å. Even when clustering is inhibited, In does not appear to perturb significantly the substrate surface. This supports the fact that the reconstruction survives to high coverages, and should again be contrasted with the rapid elimination of the substrate Ga and As surface component and of the atomic relaxation of the (110) surface under similar conditions.[25] The relative magnitude of the high-BE component is reduced with respect to the RT case. Its amplitude equals that of the metallic component at 0.5 Å. AT higher coverages, it decreases at the rate of the substrate core levels, as the layer is buried under the In overlayer. The RT clustering decreases the amount of In detected in photoemission and leads to a slow saturation of the In signal as a function of coverage. As a consequence, the metallic In component increases faster at LT than at RT. Finally, the annealing of an 8 Å overlayer at 400 °C (bottom panels of Fig. 2) causes significant clustering and metal evaporation, and enhances the reaction with the substrate. As a result, the substrate signals recover to levels comparable to the 0.5 Å In coverage case (Fig. 2). The metallic In component decreases due to the reduction in effective In coverage, and the high-BE In

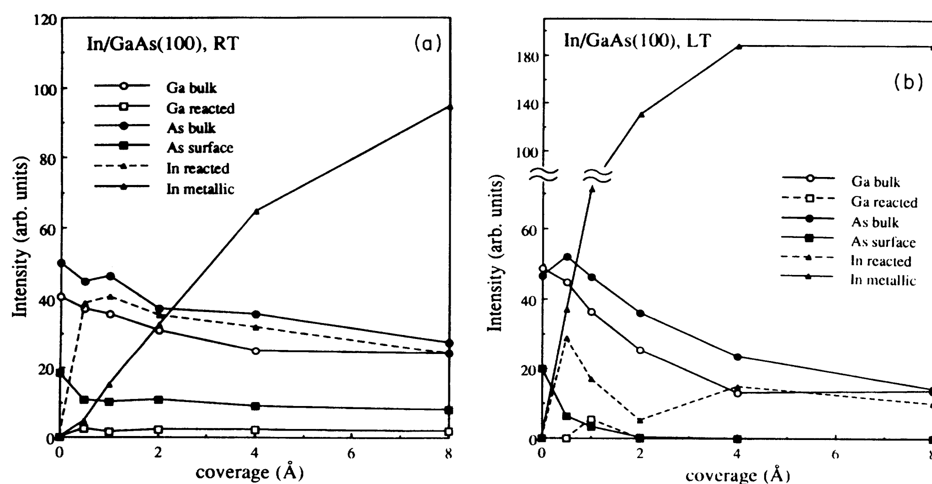

FIG. 5. Intensity of the Ga 3d, As 3d, and In 4d bulk, surface, and reacted components as a function of In coverage on (a) RT; (b) LT GaAs(100).

component increases to a level indicating the reaction of a full monolayer.

C. Au/GaAs(100)

The GaAs surface is significantly more perturbed by Au than by In. With 0.5 Å Au, the intensity of the (4×2)-$c(8\times2)$ pattern is considerably reduced. It vanishes with 1 Å Au, a rate which cannot be explained by the short inelastic mean free path of the LEED electrons only. No additional diffraction spots can be observed with Au coverages up to 16 Å. Thus, the Au overlayer is not ordered and causes significant disordering of the substrate top layers.

Figure 6(a) shows the evolution of the Ga 3*d* and As 3*d* core levels as a function of Au coverage on RT GaAs(100). The Ga and As surface components decrease rapidly and disappear with ~4 Å Au, consistent with the rapid elimination of the GaAs substrate reconstruction. At high coverages, only the As bulk component remains, and the Ga spectrum is dominated by a component at lower BE than the bulk component ($\Delta E_B=0.30$ eV). This component has been observed in numerous Au/GaAs interface studies and is generally attributed to Ga in a (Au,Ga) alloy.[27,28] The assignment, however, has never been based on solid arguments. It is well known that Ga forms an alloy with Au, but is is also understood that Ga atoms segregate to the Au surface.[29–31] The concentration of segregated Ga atoms can be large, and Ga—Ga bonding is likely to occur. Considering that the electronegativity of Au (2.54) is larger than that of As (2.18), we should expect Ga in (Au,Ga) to give up some

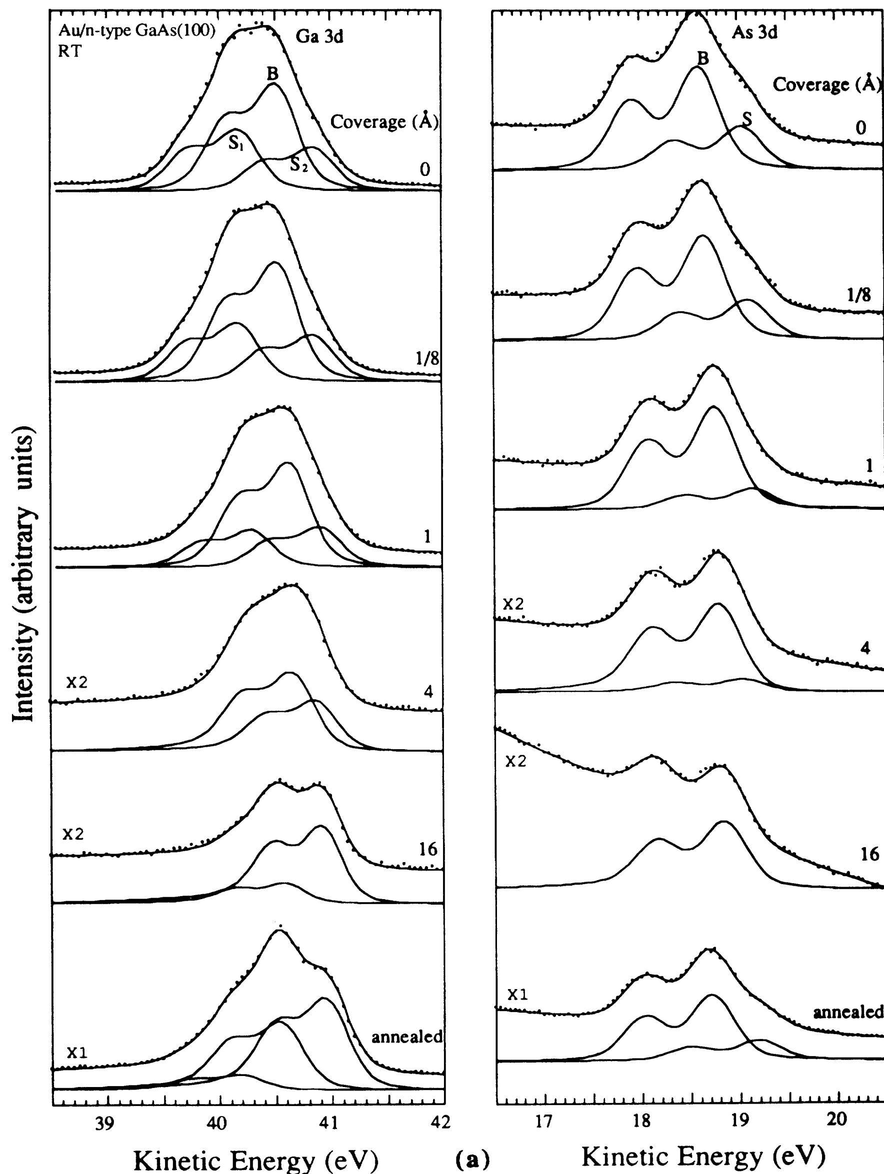

FIG. 6. Ga 3*d* and As 3*d* core levels as a function of increasing Au coverage on (a) RT and (b) LT GaAs(100). The various components are described in the text. The fitting parameters are given in Table I. The photon energy is 65 eV.

charge, resulting in a higher BE than for Ga in GaAs. Yet, the observed chemical shift is toward lower BE. The shift of this component with respect to the bulk component is exactly the same as one of the surface Ga components S_2, suggesting that its origin is more likely the emission from surface segregated Ga atoms than from the Au-Ga alloy.

Figure 6(b) shows the evolution of the Ga 3*d* and As 3*d* core levels for LT deposition. LT does not completely inhibit the reaction, as already seen with other metals at temperatures far below the one reached in this experiment.[32] Contrary to the RT case, however, the reacted Ga component is now shifted toward higher binding energy with respect to the bulk peak ($\Delta E_B = -0.65$ eV). This very broad component dominates the spectrum at high coverage. Considering the argument given above concerning the expected sign of the Ga chemical shift, we now assign this component to Ga in (Au,Ga). Its appearance at LT is explained by the fact that the Ga atoms released from the substrate are now kinetically trapped in the Au layer and undergo the charge transfer imposed by their environment. Surface segregation is reduced in this case. Given that the photon energy ensures maximum surface sensitivity, the RT signal is dominated by Ga sitting on top of Au whereas the LT signal emphasizes Ga diluted in Au. The very broad "reacted" component is a result of inequivalent sites at an overlayer-substrate interface which is far from thermodynamic equilibrium. A weak reacted As 3*d* component also appears with a binding energy ~0.55 eV higher than the bulk component, close to the binding energy of elemental As. We attribute this component to As freed by the dissolution of the GaAs surface and formation of a (Au,Ga) alloy.

The attenuation of the integrated As 3*d* signal as a function of Au coverage is shown in Fig. 5. The LT signal decays exponentially with Au coverage, indicating a quasilaminar growth of the Au layer. At RT, the attenuation deviates from the exponential line above 4 Å.

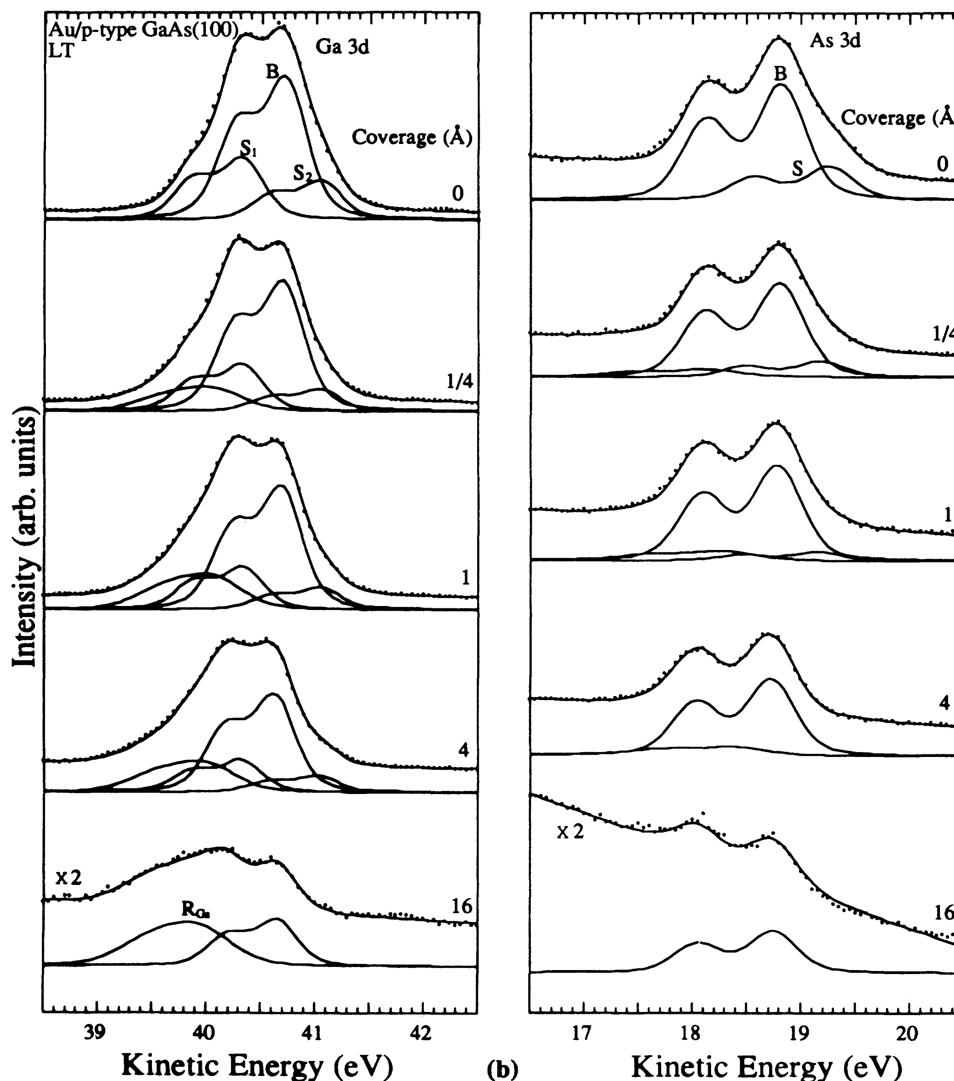

FIG. 6. (*Continued*).

Since the As line shape changes relatively little with coverage (no chemical shift), the difference between RT and LT must be due to an increase in clustering at RT and at higher coverage, rather than to the outdiffusion of As.

The intensity evolution of the core-level components [Figs. 7(a) and 7(b)] complements the results given above. At RT, all surface components decrease very fast with Au coverage, a result of the strong disruption of the substrate top and subsurface layers. The intensity of the S_2 Ga component appears to recover slightly between 4–8 Å, and to remain constant thereafter. This is due to the fortuitous coincidence in energy of this component and that attributed to Ga segregated on top of the Au layer. All integrated and bulk signals are attenuated below 4 Å at an exponential rate characterized by 5-Å inelastic mean free path, indicating a rather uniform Au layer in the early stages of the deposition. At LT, this exponential attenuation continues to much higher coverage, due to the lateral uniformity of the overlayer. The surface peaks, on the other hand, decrease somewhat slower than at RT, indicating that the surface is perturbed (dissociated) at a slower rate at LT. Finally, the intensity of the reacted Ga component initially decreases as the interface is buried under Au and then remains constant beyond 2 Å, suggesting that the outdiffusion of Ga is not totally inhibited at the temperature reached in our experiment (120 K). A limited Ga out-diffusion and alloying with Au cause the persistence of this reacted component.

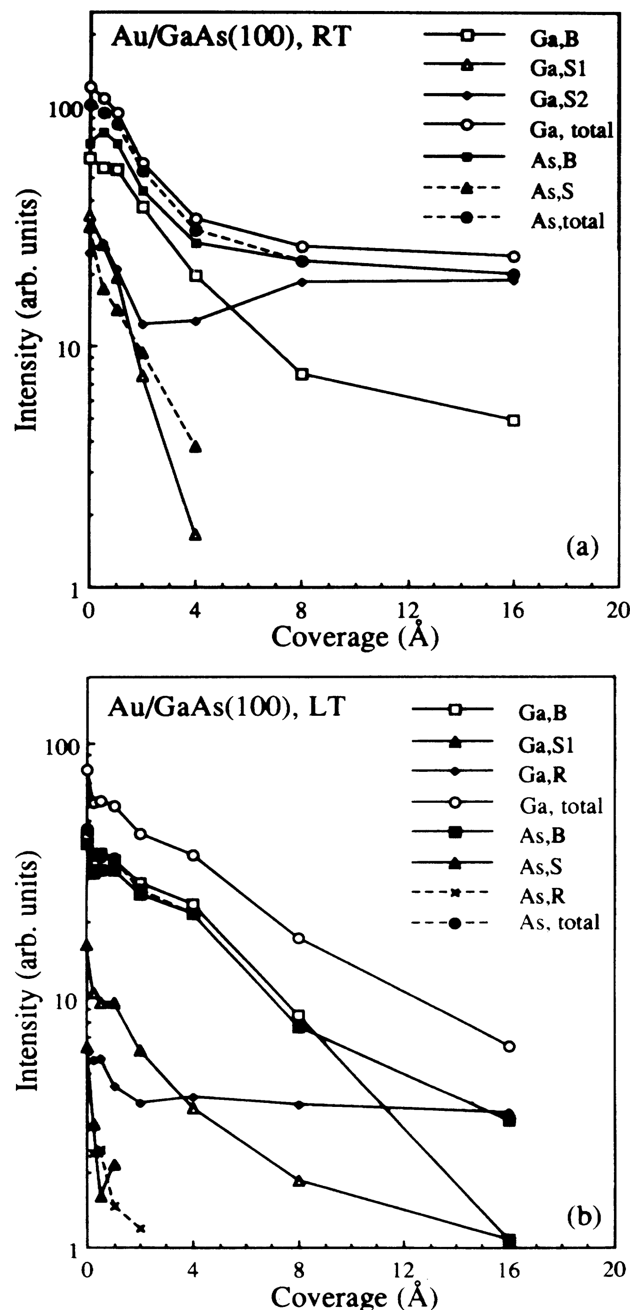

FIG. 7. Intensity of the Ga 3*d* and As 3*d* bulk, surface, and reacted components as a function of Au coverage on (a) RT; (b) LT GaAs(100).

D. Onset of overlayer metallicity

Central to the problem of Schottky barrier formation is the relationship between onset of overlayer metallicity and E_F pinning. The correlation between these two events, which has been observed on a number of interfaces between GaAs and various metals,[9,33–37] is viewed as strongly supportive of E_F pinning mechanisms based

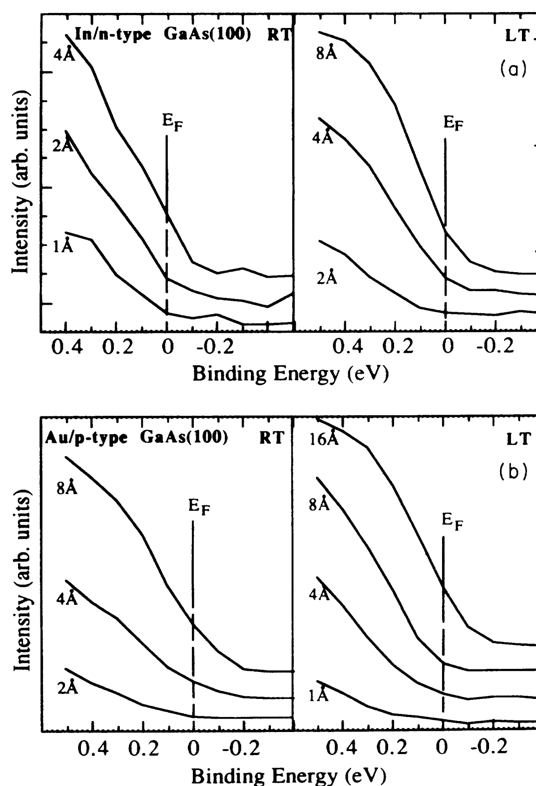

FIG. 8. The energy distribution curve around the Fermi edge with increasing metal coverages: (a) In; (b) Au.

on gap states induced or modified by the metal.[12–15,38]

This issue was investigated here for In and Au deposited at RT and at LT. Figure 8 shows the energy distribution curves near the Fermi level for the RT and LT interfaces. We assume that the onset of metallicity occurs at coverages where a sizable density of states is observed at E_F. This onset should not be viewed as the sudden appearance of a continuous and fully metallic layer, in which case E_F should bisect the cutoff edge of the photoemission spectrum.[35,39] It should rather be viewed as an indication of adatom-adatom interaction as the coverage increases, characterized by an evolution of adatom-induced gap states toward the continuum of the metallic overlayer (energy shift and broadening). This evolution should be, and indeed is, as demonstrated in the next section, accompanied by additional band bending corresponding to the new density of interface states.

At the In/GaAs interface, the onset occurs at 2–4 Å for RT depositions and at 4–8 Å for LT depositions. This difference reflects more extensive clustering at RT. In both cases, the onset occurs at higher coverage than on the (110) surface on which clustering is extensive. For the Au/GaAs interface, the onset occurs at 4–8 Å at RT, and 8–16 Å at LT.

It should be emphasized here again that surface photovoltage is not a significant factor in the measurements presented in Fig. 8. The apparent shift of the Fermi edge reflects an increase in the metallic character of the overlayer rather than a discharge of the photovoltage by charge leakage through the increasingly thick overlayer.[20] As a matter of fact, some of the measurements shown in Fig. 8 were done on p-type GaAs where photovoltage, if present, should shift the whole spectrum to higher kinetic energy. It appears therefore that full metallicity is achieved only with 3–6 ML for In and 6–10 ML for Au, surprisingly high values for both overlayers. Barring a miscalibration of the nominal coverage [the In 4d to Ga 3d photoemission peak ratios were checked against corresponding ratios recorded on LT (110) (Ref. 40) and RT (100) (Ref. 4) interfaces and found to be in good agreement], we conclude that the morphology of the overlayer, i.e., the shape and distribution of clusters on top of a probably discontinuous two-dimensional layer, has a profound influence on the development of its metallic character. In the case of the Au/[(100) GaAs] interface, this problem is compounded with extensive reaction and interdiffusion which could delay even more the onset of metallicity. In any case, the absolute coverage at which metallicity is obtained is less important for the purpose of this paper than the correlation between onset of metallicity and band bending. We show in the next section that the onset is indeed accompanied by a movement of E_F toward its final position.

E. Band bending

The movement of E_F with respect to the valence-band maximum (VBM) is obtained by monitoring the rigid shift of the Ga 3d and As 3d bulk components. The experiments are performed with negligible synchrotron-light-induced surface photovoltage, as inferred from Kelvin probe measurements. The results are plotted in Figs. 9 and 10.

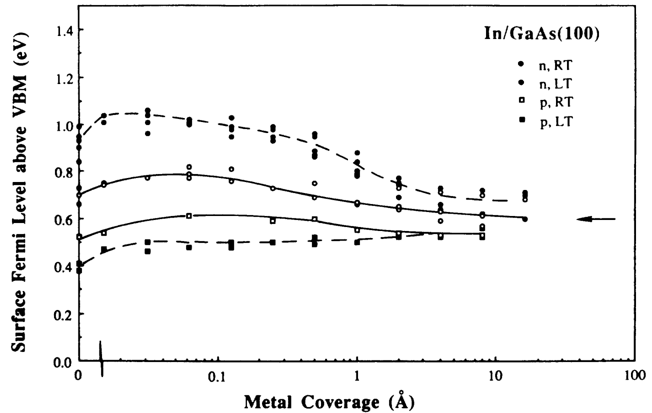

FIG. 9. E_F movement on RT and LT heavily doped n- and p-type (100) GaAs as a function of In coverage. The arrow represents the pinning position on (110) GaAs.

The initial position of E_F on the clean RT n- and p-type samples is 0.70 ± 0.05 and 0.55 ± 0.05 eV above the VBM, respectively, consistent with the results obtained by other groups.[41] The scatter in the initial position underlines the sensitivity of the initial electronic structure to the surface preparation (As decapping). The donor and acceptor states on the initial surface are due to a small density ($\sim5\times10^{12}$–10^{13} cm^{-2}) of surface defects, excess anion or cation, or imperfections resulting from the decapping procedure rather than to a large density of intrinsic states (typically a few 10^{14} cm^{-2}). Figure 9 shows that ~0.02-ML In atoms on the surface moves E_F 100–200 meV from the initial position, implying that the initial density of states cannot be significantly larger than 10^{13} cm^{-2}. Cooling to 120 K moves E_F closer to the CBM and VBM on n- and p-type samples, respectively.

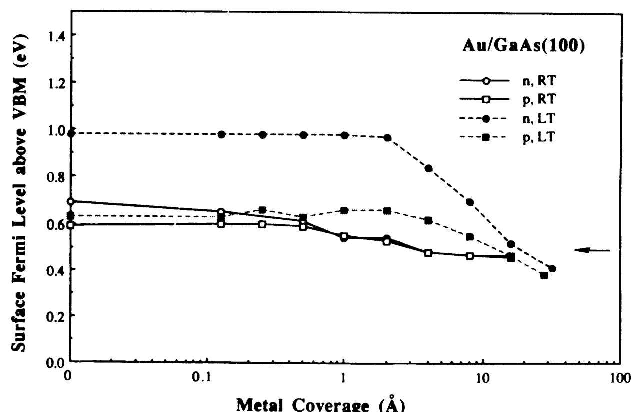

FIG. 10. Same as Fig. 9 for Au.

Except for the anomalously high initial LT E_F position in the LT Au/p-type GaAs experiment (Fig. 10), these RT and LT initial positions are reproducible and were recently confirmed in a series of experiments on Ga/GaAs(100) which will be reported elsewhere.[42] Although a small part of the RT vs LT difference can be attributed to the variation of the band gap with temperature, the main part of the shift must correspond to small but reproducible changes in the structure of these initial states.

The evolution of the band bending with metal coverages is more subtle than in the case of (110) surfaces because the pinning position is very close to the initial position. It shows, however, several important points:

First, a low coverage upward E_F movement is observed with In [and Ga (Ref. 42)], but not with Au. In introduces a density of states near or above midgap which pushes E_F on both n- and p-type samples toward the CBM. This reproducible movement is seen at RT as well as LT, although it is more pronounced at LT probably because of reduced adatom clustering. Erroneous changes in band bending due to nonequilibrium effects, i.e., SPV (Refs. 19 and 20) and surface charging,[18] or chemical shifts of the Ga $3d$ and As $3d$ core levels are ruled out. We therefore propose that, at low coverage, the isolated adatoms adsorbed on the surface introduce gap states and that the character and energy position of these states depend on the specific adatom. The energy distribution of these states can be broadened by the distribution of adatoms in inequivalent sites on the surface (both layers are atomically disordered). In analogy with models of adsorbate energy levels developed for metal/GaAs(110) interfaces,[43–45] we expect In (and Ga) to induce donor states higher in the gap than that induced by Au, in agreement with their relative first ionization energies.[9,38] In the present case, the states induced by Au are at or below the lowest E_F starting position and consequently do not produce additional band bending. The upward E_F overshoot followed by a drop toward the VBM has been observed in the past with numerous metals on p-type GaAs(110) (Refs. 9 and 46) and more recently on Si (113).[47] In the (110) case, the appearance of donor states was inferred from the LT p-type GaAs E_F movement upward from the VBM and the energy position of the states was equated to the maximum E_F position in the overshoot. These donor states were attributed to the adsorption of single adatoms or very small clusters and were particularly identifiable when clustering was inhibited during LT deposition. A key point is that the mobility of adatoms of the first deposited monolayer on the (100) surface is considerably reduced comparing to that on the (110) surface. As a result of reduced clustering, adatoms are effectively isolated at low coverage, even at RT, and an analogy can be made with the gap states induced by isolated adatoms deposited on LT (110) surfaces. Unfortunately, our present understanding of adsorption sites and adatom-induced structural changes on (100) surfaces is considerably less developed and prevents us from making further analogies on this particular point.

The second point is that the pinning positions obtained at RT and LT with In and Au are approximately 0.6 and 0.4 eV above the valence-band maximum, respectively. These numbers are in close agreement with results obtained on cleaved (110) surfaces[9,46,48] (arrows in Figs. 9 and 10) as well as on (100) surfaces prepared by direct MBE growth[7] or by As decapping.[5] Instead of the broad range of barrier heights reported by Viturro *et al*,[1,2] we observe the canonical near midgap E_F pinning with little dependence on the metal work function. With Au, it appears that the final pinning position is not yet achieved at 32 Å. However, the strong attenuation of the substrate core-level spectra and the chemical shift of the Ga $3d$ due to alloying prevent reliable measurements of band bending beyond this coverage. Comparing the E_F position at 32 Å with results obtained from thick diodes,[49] we feel it safe to assume that the final pinning is effectively achieved at 32 Å.

Third, the E_F movement toward pinning position is basically complete when metallicity is achieved in the In and Au overlayers. It occurs at higher coverage with Au than In, and at higher coverage at LT than RT, consistent with the observation and arguments given in Sec. III D. We emphasize again that all photoemission measurements were made with negligible SPV and, consequently, that high coverage E_F movements cannot be explained by the elimination of nonequilibrium effects (as in the case for low-doped samples[3]).

The E_F movement toward the pinning position starts above a few tenths of a monolayer, clearly well before metallicity is achieved in these overlayers. At these coverages, the density of defects created by chemical reactions is large enough to be detected with photoemission spectroscopy, as can be seen in Figs. 2 and 6. Thus defects cannot constitute the prime mechanism for E_F pinning. The high coverage E_F movement reflects the evolution of the adatom-induced gap states as the distance between adatoms decreases and the adatom-substrate interaction is increasingly affected by the adatom-adatom interaction (see the development of the metallic In peak in Fig. 2). This interaction eventually leads to a metallic overlayer. We suggest, therefore, that the prime pinning mechanism here again corresponds to the existence of a continuum of metallic states which induce states in the semicondutor gap. These metal-induced gap states necessarily interact with the states of the initial surface as well as with the defect states introduced by the chemistry of the interface, but plays a dominant role in the establishment of the barrier.

V. CONCLUSION

We have used synchrotron-radiation photoemission spectroscopy to investigate interfaces between In and Au and MBE-grown GaAs(100) surfaces prepared by removal of a protective As layer in UHV. Beyond the details of the chemistry and morphology of these two very different interfaces, we have provided a comprehensive investigation of metal-induced band bending on (100) surfaces where photoemission-induced surface photovoltage and other nonequilibrium phenomena are not significant. Regarding the mechanisms responsible for the formation of the Schottky barrier, the results shown in this paper

support the general ideas developed in previous work on (110) surfaces,[9,33–35,37,38,46] even though some of the previous results were partially influenced by surface photovoltage. These ideas emphasize the role of (1) adsorbate-induced gap states at low coverage, when adatoms are isolated or distributed in small clusters on the surface; (2) gap states induced or modified by the metal when the overlayer becomes metallic. The Fermi level pinning positions with In and Au are about 0.2 eV apart, consistent with positions found on cleaved (110) surfaces.

ACKNOWLEDGMENTS

This work was supported by a grant form the National Science Foundation (No. DMR-9018521). The assistance of the staff of the NSF-supported Synchrotron Radiation Center is gratefully acknowledged. We would like to thank Dr. L.J. Brillson, Dr. S. Chang, Dr. I. M. Vitomirov, and Dr. C. Palmstrom for very valuable discussions on As decapping. CMRC2 is "Unité Associee au Centre National de la Recherche Scientifique."

[1]R. E. Viturro, S. Chang, J. L. Shaw, C. Mailhiot, L. J. Brillson, A. Terrasi, Y. Hwu, G. Margaritondo, P. D. Kirchner, and J. M. Woodall, J. Vac. Sci. Technol. B **7**, 1007 (1989).
[2]R. E. Viturro, C. Mailhiot, J. L. Shaw, L. J. Brillson, D. Lagraffe, G. Margaritondo, G. D. Pettit, and J. M. Woodall, J. Vac. Sci. Technol. A **7**, 855 (1989).
[3]D. Mao, G. LeLay, Y. Hwu, G. Margaritondo, M. Santos, M. Shayegan, L. T. Florez, J. P. Harbison, and A. Kahn, J. Vac. Sci. Technol. B **9**, 2083 (1991).
[4]C. J. Spindt, R. Cao, K. E. Miyano, I. Lindau, W. E. Spicer, and Y. C. Pao, J. Vac. Sci. Technol. B **8**, 974 (1990).
[5]C. J. Spindt, M. Yamada, P. L. Meissner, K. Miyano, A. Herrera, A. J. Arko, and W. E. Spicer, J. Vac. Sci. Technol. B **9**, 2090 (1991).
[6]S. Chang, I. M. Vitomirov, L. J. Brillson, D. F. Rioux, P. D. Kirchner, G. D. Pettit, and J. M. Woodall, J. Vac. Sci. Technol. B **9**, 2129 (1991).
[7]S. P. Wilks, J. I. Morris, D. A. Woolf, and R. H. Williams, J. Vac. Sci. Technol. B **9**, 2118 (1991).
[8]W. E. Spicer, P. W. Chye, P. R. Skeath, C. Y. Su, and I. Lindau, J. Vac. Sci. Technol. **16**, 1427 (1979).
[9]A. Kahn, K. Stiles, D. Mao, S. F. Horng, K. Young, J. McKinley, D. G. Kilday, and G. Margaritondo, in *Metallization and Metal-Semiconductor Interfaces,* edited by I. Batra (Plenum, New York, 1989), p. 163.
[10]W. E. Spicer, Appl. Surf. Sci. **41/42**, 1 (1989).
[11]L. J. Brillson, Surf. Sci. Rep. **2**, 123 (1982).
[12]V. Heine, Phys. Rev. **138**, 1689 (1965).
[13]F. Flores and C. Tejedor, J. Phys. C **20**, 145 (1987).
[14]J. Tersoff, Phys. Rev. Lett. **52**, 465 (1984).
[15]R. Ludeke, Phys. Rev. B **40**, 1947 (1989).
[16]J. L. Freeouf, J. M. Woodall, L. J. Brillson, and R. E. Viturro, Appl. Phys. Lett. **56**, 69 (1990).
[17]M. H. Hecht, Phys. Rev. B **41**, 7918 (1990).
[18]M. Alonso, R. Cimino, and K. Horn, Phys. Rev. Lett. **64**, 1947 (1990); J. Vac. Sci. Technol. A **9**, 891 (1991).
[19]D. Mao, A. Kahn, M. Marsi, and G. Margaritondo, Phys. Rev. B **42**, 3228 (1990).
[20]D. Mao, A. Kahn, M. Marsi, and G. Margaritondo, J. Vac. Sci. Technol. A **9**, 898 (1991).
[21]For a comprehensive review on photoemission curve fitting, see J. J. Joyce, M. Del Giudice, and J. H. Weaver, J. Electron Spectrosc. Relat. Phenom. **49**, 31 (1989).
[22]S. Doniach and M. Šunjić, J. Phys. C **3**, 285 (1970).
[23]P. Drathen, W. Ranke, and K. Jacobi, Surf. Sci. **77**, L162 (1978).
[24]G. Le Lay, D. Mao, Y. Hwu, G. Margaritondo, and A. Kahn, Phys. Rev. B **43**, 14 301 (1991).
[25]K. Stevens, L. Soonckindt, and A. Kahn, J. Vac. Sci. Technol. A **8**, 2068 (1990).
[26]K. K. Chin, T. Kendelewicz, N. Newman, I. Lindau, and W. E. Spicer, J. Vac. Sci. Technol. B **4**, 955 (1986).
[27]W. G. Petro, T. Kendelewiz, I. Lindau, and W. E. Spicer, Phys. Rev. B **34**, 7089 (1986).
[28]J. J. Joyce, M. Grioni, M. del Giudice, M. W. Ruckman, F. Bosherini, and J. H. Weaver, J. Vac. Sci. Technol. A **5**, 2019 (1987).
[29]Y. Shapira, L. J. Brillson, A. D. Katnani, and G. Margaritondo, Phys. Rev. B **30**, 4586 (1984).
[30]F. Xu, Y. Shapira, D. M. Hill, and J. H. Weaver, Phys. Rev. B **35**, 7417 (1987).
[31]P. W. Chye, I. Lindau, P. Pianetta, C. M. Garner, C. Y. Su, and W. E. Spicer, Phys. Rev. B **18**, 5545 (1978).
[32]G. D. Waddill, C. M. Aldao, I. M. Vitomirov, S. G. Anderson, C. Capasso, and J. H. Weaver, J. Vac. Sci. Technol. B **7**, 950 (1989).
[33]D. Mao, K. Young, K. Stiles, and A. Kahn, J. Appl. Phys. **64**, 4777 (1988).
[34]M. Prietsch, M. Domke, C. Laubschat, and G. Kaindl, Phys. Rev. Lett. **60**, 436 (1988).
[35]K. Stiles and A. Kahn. Phys. Rev. Lett. **60**, 440 (1988).
[36]M. Prietsch, M. Domke, C. Labschat, T. Mandel, C. Xue, and G. Kaindl, Z. Phys. B **74**, 21 (1989).
[37]M. Prietsch, M. Domke, C. Laubschat, G. Remmers, E. Weschke, T. Mandel, J. E. Ortega, and G. Kaindl, J. Vac. Sci. Technol. B **7**, 986 (1989).
[38]W. Mönch, J. Vac. Sci. Technol. B **6**, 1270 (1988).
[39]K. Stiles and A. Kahn, Phys. Rev. Lett. **62**, 606 (1989).
[40]D. Mao, L. Soonckindt, G. Margaritondo, and A. Kahn (unpublished).
[41]S. P. Svensson, J. Kanski, T. G. Andersson, and P. -O. Nilsson, J. Vac. Sci. Technol. B **2**, 235 (1984), and references therein.
[42]D. Mao, Y. Hwu, G Margaritondo, M. Santos, M. Shayegan, and A. Kahn (unpublished).
[43]W. Mönch, Europhys. Lett. **63**, 275 (1988).
[44]J. E. Klepeis and W. A. Harrison, J. Vac. Sci. Technol. B **7**, 964 (1989).
[45]I. Lefebvre, M. Lanoo, and G. Allan, Europhys. Lett. **10**, 359 (1989).
[46]K. Stiles, A. Kahn, D. G. Kilday, and G. Margaritondo, J. Vac. Sci. Technol. B **5**, 987 (1987).
[47]P. Althainz, U. Myler and K. Jacobi, Phys. Rev. B **43**, 14 157 (1991).
[48]R. Cao, K. Miyano, T. Kendelewicz, K. K. Chin, I. Lindau, and W. E. Spicer, J. Vac. Sci. Technol. B **5**, 998 (1987).
[49]N. Newman, W. E. Spicer, T. Kendelewicz, and I. Lindau, J. Vac. Sci. Technol. B **4**, 931 (1986).

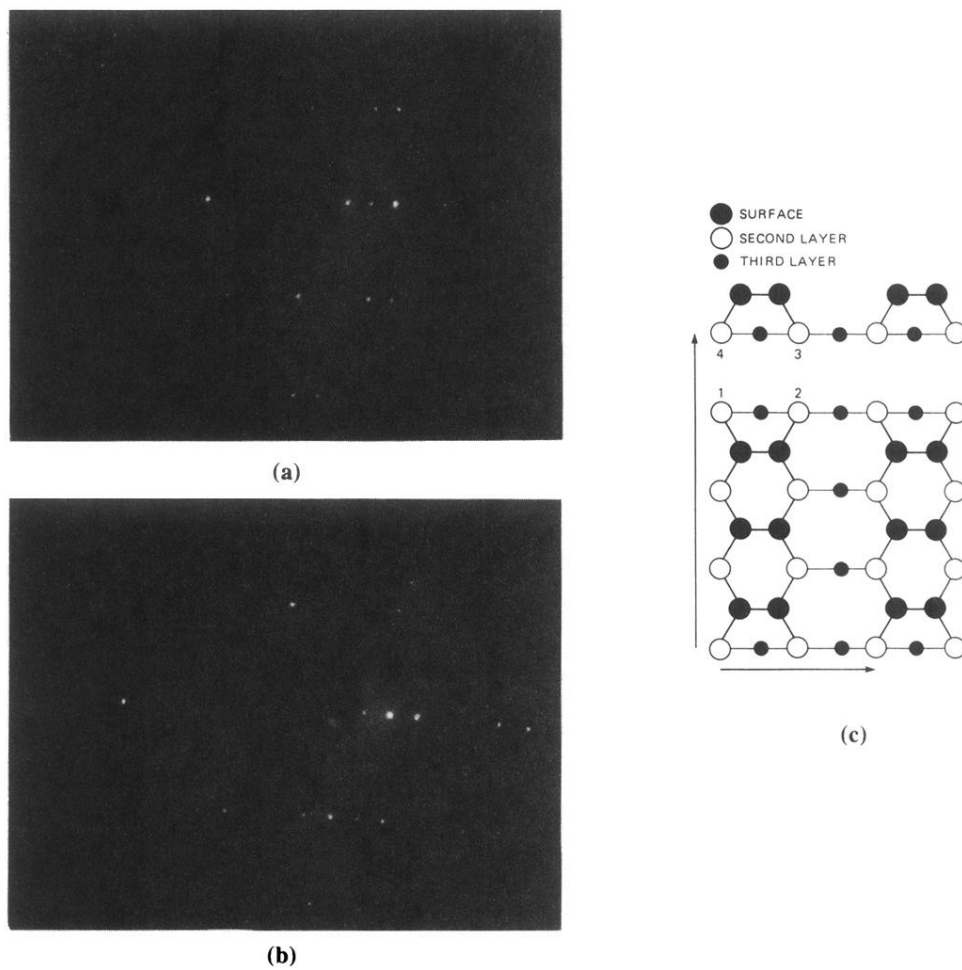

FIG. 1. LEED patterns from the decapped (100) GaAs surface: (a) 500 °C anneal, 70 eV, (b) 555 °C anneal, 60 eV, (c) a schematic of a missing Ga-dimer row model of the (4×2) reconstruction; open and solid circles represent As and Ga atoms, respectively.